

# Origin of branch points in the spectrum of $PT$ -symmetric periodic potentials

Ching-Hao Chang, Shi-Ming Wang, and Tzay-Ming Hong

*Department of Physics, National Tsing Hua University, Hsinchu 30043, Taiwan, Republic of China*

(Dated: November 8, 2018)

There exists multiple branch points in the energy spectrum for some  $PT$ -symmetric periodic potentials, where the real eigenvalues turn into complex ones. By studying the transmission amplitude for a localized complex potential, we elucidate the physical origin of the breakdown of perturbation method and Born approximation. Mostly importantly, we derive an analytic criteria to determine why, when and where the bifurcation will occur.

PACS numbers: 03.65.Ge, 03.65.Nk, 11.30.Er

## I. INTRODUCTION

Non-Hermitian (NH) quantum mechanics (QM) has been used to describe an open system because complex eigenenergies imply the existence of a sink or source for the particle. The  $PT$ -symmetric hamiltonian is a special case in NHQM that can exhibit entirely real spectra[1]. Its development has gone through various stages[2] with applications ranging from quantum cosmology[3], quantum field theory[4] to quantum computation[5, 6]. A flourishing example is in connection with the optical lattice which can be simulated by the Schrödinger equation. This provides a fertile ground to test the NH-related concepts experimentally. In this spirit scientists have studied the  $PT$ -symmetric periodic potentials and investigated several interesting features: (1) The existence of several branch points which demarcate the real and complex spectra[7]. (2) Optical soliton solutions are found within the energy gap with real eigenvalues[8]. (3) A quantum phase transition is identified when a sufficiently large real periodic potential is superimposed to render all the spectrum real[9]. The latter two, which provide the basis for the fruitful beam dynamics[8, 9], are closely related to the branch point and bifurcation feature. Although the branch points and a complex spectrum have been attributed to the failure of perturbation expansion[10], we believe it is worthwhile to study in more detail the physical origin of this failure.

We shall start by studying a localized imaginary potential before embarking on the more interesting periodic case. Several new features are discussed in Section II which include (1) Existence of an upper bound for the imaginary part of eigenenergies. (2) Breakdown of the Born approximation for scattering states unless a large enough real potential is added. (3) Fano resonance within the imaginary barrier can cause the transmission amplitude to become huge by repetitive enhancements. (4) An incoming wave packet will also exhibit special features when its momentum is near the resonance. We find that the size of the transmission amplitude is the key to features (2) and (3). In Section III we argue that the spectrum of the  $PT$ -symmetric periodic potential is predominantly shaped by the transmission amplitude for a single unit cell. Therefore, the conclusions in Section II

for a localized potential are still applicable in the periodic case. By use of the Bloch's theorem, we derive an analytic criteria for the occurrence of branch point and the band structure bifurcation. Discussions and conclusions are arranged in the final Section IV.

## II. SINGLE IMAGINARY SQUARE POTENTIAL

### A. Localized states

At first glance, one might think that the eigenenergies of a complex potential are most likely also complex. This is in fact not true. For instance, take an imaginary square potential  $iV_0$  from  $x = 0$  to  $x = a$  where  $V_0 > 0$  and zero potential elsewhere. It exhibits both real/imaginary eigenvalues, which are continuous/discrete and correspond to scattering/localized states, respectively.

Since the barrier potential is symmetric with respect to  $x = a/2$ , the spatial part of the localized wavefunction,  $\psi(x, t) = \phi(x)e^{-iEt}$  where  $\hbar$  has been set to unity for convenience, can be expressed as:

$$\phi(x) = \begin{cases} \pm e^{-(ik-q)(x-a/2)}, & x \leq 0, \\ A(e^{ip(x-a/2)} \pm e^{-ip(x-a/2)}), & 0 \leq x \leq a, \\ e^{(ik-q)(x-a/2)}, & x \geq a \end{cases} \quad (1)$$

where momentum  $k$  and  $q$  are real and positive,  $p$  is complex, and the  $\pm$  sign denotes respectively the even/odd-parity state with respect to  $x = a/2$ . The minus sign in the exponent of  $\phi(x \leq 0)$  is to prevent it from blowing up at  $x \rightarrow -\infty$ . These momenta are related by the complex energy  $E$ :

$$E = \frac{-(ik-q)^2}{2m} = \frac{p^2}{2m} + iV_0. \quad (2)$$

One should be aware that the standard concept of density current need not survive[11] the transition to NHQM. For instance, in the case of a  $PT$ -symmetric potential  $j(x, t)$  has to be redefined as  $-i[\psi^*(x, t)\partial\psi(-x, t)/\partial x - \psi(-x, t)\partial\psi^*(x, t)/\partial x]/2m$  in order to obtain the continuity equation. For the sake of arguments, let us stick to the standard notion and deduce the following mathematical equation from the Schrödinger equation for a general

complex potential  $V(x)$ :

$$2\text{Im}V(x)|\psi(x,t)|^2 = \frac{\partial}{\partial t}|\psi(x,t)|^2 + \frac{\partial}{\partial x}j_0(x,t) \quad (3)$$

where the symbol  $\text{Im}$  denotes taking the imaginary part and  $j_0(x,t) \equiv -i[\psi^*(x,t)\partial\psi(x,t)/\partial x - \psi(x,t)\partial\psi^*(x,t)/\partial x]/2m$ . Integrating over the whole space gives

$$\int_{-\infty}^{\infty} dx \frac{\partial}{\partial t}|\psi(x,t)|^2 = 2 \int_{-\infty}^{\infty} dx \text{Im}V(x)|\psi(x,t)|^2 \quad (4)$$

where  $j_0(x,t)$  vanishes at  $x = \pm\infty$  for the localized state in Eq.(1). This leads to the following inequality

$$\text{Im}E \int_{-\infty}^{\infty} dx |\psi(x,t)|^2 < \text{Max}(\text{Im}V) \int_{-\infty}^{\infty} dx |\psi(x,t)|^2 \quad (5)$$

which tells us that the height of the imaginary barrier  $V_0$  serves as an upper bound for  $\text{Im}E$ :

$$0 \leq \text{Im}E < V_0. \quad (6)$$

By matching the boundary conditions, we can further show that the number of these localized states is finite and their energies are discrete. In contrast to being zero for a real well, the current density  $j(x,t)$  is not only nonvanishing, but also quantized for an imaginary barrier/well:

$$j_n(x,t) = \frac{k_n}{m} e^{-2q_n|x-a/2|+2\text{Im}E_n t} \quad (7)$$

where  $n$  labels these discrete localized states.

All the derivations so far are based on the assumption that  $V_0 > 0$ . However, it is easy to generalize to an imaginary well. The action of changing the potential from  $iV_0$  to  $-iV_0$  is equivalent to reversing the time, which transforms the hydrant-like bound state into a sink. The same conclusion applies to the eigenfunctions and eigenenergies after we take the complex conjugate of the time-independent Schrödinger equation. As a result, the upper bound in Eq.(6) needs to be modified as

$$-V_0 < \text{Im}E \leq 0. \quad (8)$$

## B. Scattering states

Another interesting problem is to study the transmission and reflection coefficients for a complex square barrier. This is relevant to our discussion of the spectrum for a periodic potential in Section III. The scattering state takes the form:

$$\phi_{r,k}(x) = \begin{cases} e^{ikx} + r e^{-ikx}, & x \leq 0, \\ A e^{i(p-iq)x} + B e^{-i(p-iq)x}, & 0 \leq x \leq a, \\ t e^{ikx}, & x \geq a \end{cases} \quad (9)$$

where subscript  $r$  is to distinguish this right-moving state from its degenerate state  $\phi_{l,k}(x)$  that travels in the opposite direction. Fitting the boundary conditions, we find

$$t = \frac{-4kk'e^{-ika}}{e^{i(k+k')a}(k-k')^2 - e^{i(k-k')a}(k+k')^2} \quad (10)$$

$$r = \frac{2i(k^2 - k'^2) \sin(k'a) e^{-ika}}{e^{i(k+k')a}(k-k')^2 - e^{i(k-k')a}(k+k')^2} \quad (11)$$

where  $k' \equiv p - iq$  is the complex momentum inside the barrier. The amplitude  $t$  in Eq.(9) consists of contributions from all paths that reflect inside the barrier arbitrary number of times:

$$t = t_1 t_2 e^{ik'a} + t_1 r_2 r_1 t_2 e^{3ik'a} + t_1 r_2 r_1 r_2 r_1 t_2 e^{5ik'a} + \dots \quad (12)$$

where  $t_{1,2}/r_{1,2}$  denote the transmission/reflection amplitudes at the boundaries  $x = 0$  and  $x = a$ , respectively. The higher-order terms in Eq.(12) converge to zero for a real barrier. But this is no longer true for a positive imaginary barrier because the longer they stay in the source the more probability they can gain. As a result, the values of resonance peaks can be much bigger than unity, and the Born approximation that neglects the higher-order terms is expected to break down. These two features are clearly shown in Fig.1 and the number of resonances and their peak values increase when we raise  $V_0$  in Fig.2.

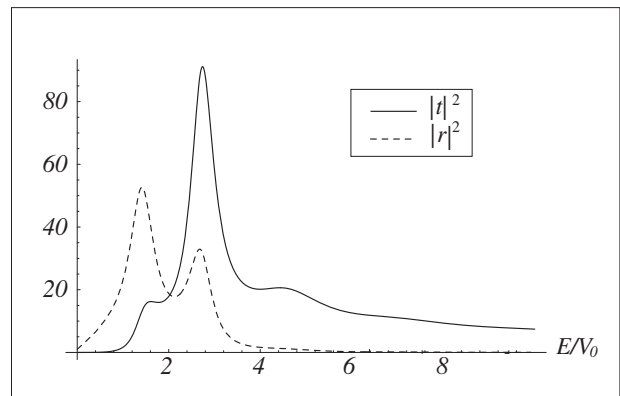


FIG. 1: Set the effective mass of electron as  $m = 0.5$ . The transmission and reflection coefficients of an imaginary barrier with height  $V_0 = 5$  and width  $a = 2$  are plotted as a function of  $E/V_0$  where  $E$  represents the energy of the scattering state.

Another important issue of the scattering process is the interference condition for Fano resonance. In real barriers, the resonance in transmission results from the constructive interference between different scattering paths shown in Eq.(12), which gives the familiar condition  $a = n\lambda/2 \equiv n\pi/p$ . In the mean time, reflection peaks are attributed to the destructive interference when

$$a = (n + \frac{1}{2}) \frac{\lambda}{2} \quad (13)$$

is satisfied. These two conditions become more complicated for an imaginary potential because the phase shift

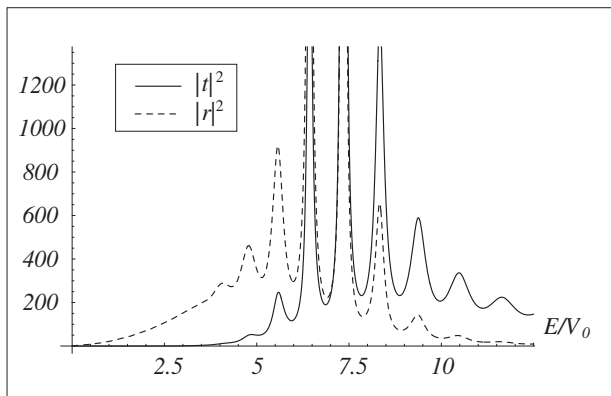


FIG. 2: Same as Fig.1 except the barrier height is increased by eight folds to  $V_0 = 40$ .

$E$	223.6	257.4	294.1	333.4
$ t ^2$	247.5	2322.5	24485.9	1507.7
$n$	13.52	14.49	15.48	16.47

TABLE I: Partial list of the energies and peak values of the transmission coefficient in Fig.2 and their corresponding  $n$  defined by  $n = 2a/\lambda$ .

due to reflections from the boundaries between the imaginary and real potential regimes is energy-dependent. The amplitude  $r_{1,2}$  in Eq.(12) can be determined by studying the reflection by an imaginary step potential of height  $iV_0$ :

$$r_{1,2} = \frac{k - k'}{k + k'} \simeq \begin{cases} 1, & E \ll V_0 \\ iV_0/4E, & E \gg V_0 \end{cases} \quad (14)$$

which shows that there is an additional phase shift ranging from 0 to  $\pi/2$  as  $E$  increases. It is straightforward to write down an equation similar to Eq.(12) for the reflection amplitude,  $r$ . Since both equations are geometric series with the same common ratio,  $r_1 r_2 \exp(2ik'a)$ , it is expected that the transmission and reflective resonances for an imaginary barrier should all follow the same second criterion, Eq.(13), at the limit  $E \gg V_0$ . To verify these interference features, a partial list of the energies, peak values of the transmission coefficient and corresponding  $n$  in Fig.2 are numerically calculated and summarized in Tab. I. For an imaginary well, Eq.(14) remains valid after  $V_0$  is replaced by  $-V_0$ . However, the resonance peaks are no longer pronounced because the sink now draws in probability as the wave reflects in the well.

In order to facilitate the discussion of a  $PT$ -symmetric periodic potential in Section III, let us put the square barrier and well side by side to form a simple  $PT$ -symmetric potential. The perturbation expansion can be shown to still break down as in the periodic case[9]. The similarity goes further that the perturbation in both potentials can be salvaged by incorporating a big-enough real potential. On the other hand, we can ask how strong a complex potential can ruin the perturbation expansion.

Take this pair of square barrier and well potential,  $V(x) = \{U_0[\Theta(x+a) - \Theta(x-a)] + iV_0[\Theta(x+a) - \Theta(x)] - iV_0[\Theta(x) - \Theta(x-a)]\}$ , for example. The threshold for  $V_0$  is determined when the maximum of the common ratio in Eq.(12) equals 1; namely,

$$|r_1 r_2 \exp(2ik'a)|_{E=0} = 1 \quad (15)$$

where

$$\begin{aligned} r_1 &= \frac{\sqrt{E} - \sqrt{E - U_0 - iV_0}}{\sqrt{E} + \sqrt{E - U_0 - iV_0}} \\ r_2 &= \frac{\sqrt{E - U_0 - iV_0} - \sqrt{E - U_0 + iV_0}}{\sqrt{E - U_0 - iV_0} + \sqrt{E - U_0 + iV_0}} \\ k' &= \sqrt{2m(E - U_0 - iV_0)}. \end{aligned} \quad (16)$$

For the parameters  $m = 0.5$ ,  $a = 1$  and  $U_0 = 50$ , this critical  $V_0$  equals 0.00136. Numerical calculations show that this is the same threshold for the transmission amplitude to exceed 1, which shall be proved in Section III to be the harbinger for the bifurcation of spectrum for the  $PT$ -symmetric periodic potential.

### C. Evolution of a wave packet through the imaginary barrier

When a wave packet impinges on a real potential barrier, the resonances are not critical to its evolution since their transmission amplitude is of the same order as the nonresonant ones. However, as is shown in Tab. I, the resonant amplitudes can reach a few tens of a thousand for an imaginary barrier. It is, therefore, of interest to study how a wave packet progresses through such a potential.

As usual, we first decompose it into the scattering states  $\phi_k$  in Eq.(9) and the localized states  $\phi_n$  in Eq.(1):

$$\Psi(x, t = 0) = \sum_k C_k \phi_k^R(x, 0) + \sum_n C_n \phi_n^R(x, 0) \quad (17)$$

where the superscript  $R$  denotes the right eigenstate. This is similar to the case of nonHermitian matrices, for which the right and left eigenstates may not be the same. Since they can exhibit different physical properties and time evolution, it is important to distinguish them. Take the imaginary square potential, for instance. The barrier seen by the right eigenstates in Eqs.(9) and (1) will turn into a well for their left counterparts, which are defined by

$$\langle \phi_{k/n}^L | \hat{H} = \langle \phi_{k/n}^L | E_{k/n} \quad (18)$$

or

$$\left\{ \frac{\hat{p}^2}{2m} - iV_0[\Theta(x) - \Theta(x-a)] \right\} \phi_{k/n}^L = E_{k/n}^* \phi_{k/n}^L \quad (19)$$

when expressed in the real space. These two eigenstates obey the following orthogonality relation

$$\langle \phi_{k/n}^L | \phi_{k'/n'}^R \rangle = \langle \phi_{k/n}^L | \phi_{k'/n'}^R \rangle \delta_{k/n, k'/n'}. \quad (20)$$

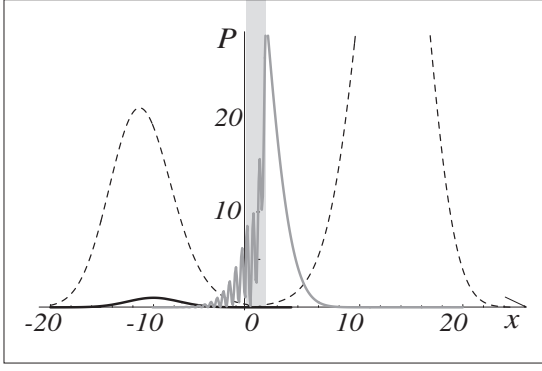


FIG. 3: The evolution of the wave packet in Eq.(22) impinges on an imaginary square barrier in the gray area with parameters described in the text. The solid, gray, and dashed lines represent the distribution at  $t = 0, 2$ , and  $5$ , respectively.

By use of the above relation and the general product,  $c$  method, introduced by Gilary *et al.*[12], the weightings  $C_k, C_n$  in Eq.(17) can be determined as

$$C_{k/n} = \frac{\int [\phi_{k/n}^L(x)]^* \Psi(x, t=0) dx}{\int [\phi_{k/n}^L(x)]^* \phi_{k/n}^R(x) dx} \quad (21)$$

The initial wave packet,  $\Psi(x, 0)$ , is chosen as a harmonic coherent state:

$$\Psi(x, 0) = \left(\frac{2b}{\pi}\right)^{\frac{1}{4}} e^{-b(x-x_0)^2 + ip_0(x-x_0)} \quad (22)$$

where  $x_0$  and  $p_0$  denote the position and momentum of the center of the packet, while  $1/2\sqrt{b}$  is its mean width. For an imaginary square barrier of height  $V_0 = 5$ , the evolution of wave packet is illustrated in Fig.3 with  $(x_0, b) = (-10, 0.08)$  and  $p_0 = 5.23$  chosen to be near one of the resonance peaks in Fig.1. It can be seen that the amplitude gets enhanced upon entering the imaginary barrier due to the resonance. The oscillatory behavior only exists at intermediate time, as depicted by the gray line. As the wave packet exits the barrier, the amplitudes of both transmitted and reflected waves have already been enhanced by 55 and 20 times each.

### III. $PT$ -SYMMETRIC PERIODIC POTENTIAL

#### A. Origin of bifurcation

In the following, we generalize the single imaginary potential to a  $PT$ -symmetric periodic one. Set the unit cell in  $-d/2 \leq x \leq d/2$  and denote the eigenfunction by

$$\Phi(x) = \phi_{r,k}(x) + A\phi_{l,k}(x) \quad (23)$$

where  $\phi_{r,k}(x)$  and  $\phi_{l,k}(x)$  are the right- and left-moving scattering states in the unit cell similar to Eq.(9). According to the Bloch's theorem, the wavefunction in its

previous cell  $-3d/2 \leq x \leq -d/2$  can be represented as:

$$\Phi(x) = e^{-iKd} [\phi_{r,k}(x+d) + A\phi_{l,k}(x+d)] \quad (24)$$

where  $K$  is the Bloch wave number. Matching the boundary conditions at  $x = -d/2$  gives

$$\begin{aligned} \phi_{r,k}\left(-\frac{d}{2}\right) - e^{-iKd}\phi_{r,k}\left(\frac{d}{2}\right) &= A[e^{-iKd}\phi_{l,k}\left(\frac{d}{2}\right) - \phi_{l,k}\left(-\frac{d}{2}\right)] \\ \phi'_{r,k}\left(-\frac{d}{2}\right) - e^{-iKd}\phi'_{r,k}\left(\frac{d}{2}\right) &= A[e^{-iKd}\phi'_{l,k}\left(\frac{d}{2}\right) - \phi'_{l,k}\left(-\frac{d}{2}\right)] \end{aligned} \quad (25)$$

where  $\phi'$  denotes  $d\phi/dx$ . By use of the equality  $[\phi_{r,k}\phi'_{l,k} - \phi'_{r,k}\phi_{l,k}]|_{x=-d/2}^{x=d/2} = 0$ , the above equations require the following condition in order to have a nonzero  $A$ :

$$\frac{U_1 - U_2}{2[\phi_{r,k}\phi'_{l,k} - \phi'_{r,k}\phi_{l,k}]|_{x=d/2}} = \cos Kd \quad (26)$$

where

$$U_1 = \phi_{r,k}\left(-\frac{d}{2}\right)\phi'_{l,k}\left(\frac{d}{2}\right) + \phi_{r,k}\left(\frac{d}{2}\right)\phi'_{l,k}\left(-\frac{d}{2}\right)$$

and the definition of  $U_2$  is similar but with the subindices  $r$  and  $l$  interchanged. Equation (26) gives us the dispersion relation for the spectrum.

Let us write down the form of  $\phi_{r,l}$  at  $x = \pm d/2$  explicitly

$$\begin{aligned} \phi_{r,k}(x) &= \begin{cases} e^{ikx} + R_r e^{-ikx}, & x = -\frac{d}{2} \\ T e^{ikx}, & x = \frac{d}{2} \end{cases} \\ \phi_{l,k}(x) &= \begin{cases} T e^{-ikx}, & x = -\frac{d}{2} \\ e^{-ikx} + R_l e^{ikx}, & x = \frac{d}{2} \end{cases} \end{aligned} \quad (27)$$

where the amplitudes  $R, T$  may vary with  $k$ . Inserting them in Eq.(26) gives the relation between the energy  $E = k^2/2m$  and  $K$  for a general periodic potential:

$$\frac{T^2 - R_r R_l}{2T} e^{ikd} + \frac{1}{2T} e^{-ikd} = \cos Kd. \quad (28)$$

The fact that we are interested at the branch points of  $PT$ -symmetric periodic potentials allows us to further simplify Eq.(28). First, take the complex conjugate of the Schrödinger equation for  $\phi_r$

$$\left[\frac{-1}{2m} \frac{d^2}{dx^2} + V^*(x)\right] \phi_{r,k}^*(x) = E^* \phi_{r,k}^*(x). \quad (29)$$

If we choose the unit cell to also exhibit the  $PT$ -symmetry, the potential  $V^*(x)$  will become identical to  $V(-x)$ . Furthermore,  $E^*$  is the same as  $E$  since the eigenenergy is real at the branch point. These two properties combined with Eq.(29) tell us that  $\phi_{r,k}^*(x)$  must be a linear combination of the two scattering states:

$$\phi_{r,k}^*(x) = B\phi_{l,k}(-x) + C\phi_{r,k}(-x). \quad (30)$$

This relation gives four equations, each of which corresponds to matching the right- and left-moving part of the wavefunctions on either side of the unit cell:  $R_r^* = B$ ,  $1 = BR_l + CT$ ,  $0 = BT + CR_r$  and  $T^* = C$ . It is straightforward to show that they yield  $T^* = T/(T^2 - R_r R_l)$  which simplifies Eq.(28) to:

$$\frac{1}{|T|} \cos(kd + \theta) = \cos Kd \quad (31)$$

where  $\theta$  is the phase of  $T$ . If  $|T|$  should ever be larger than 1 near the extrema of the LHS in Eq.(31), there will be no real solution for those  $K$  that make  $|\cos Kd|$  large. In other words, the eigenenergies near the Brillouin zone boundaries of  $K$  are sure to be complex. We emphasize that the condition that  $|T|$  exceeds unity for some  $k$  alone is not enough to predict the bifurcation. It has to coincide with the occurrence of extreme values for  $\cos(kd + \theta)/|T|$ . This is complement to the previous conclusion[10] that perturbation forbids bifurcation. What we have shown here is that  $|T| \leq 1$  guarantees there will be no bifurcation. It is then natural to ask whether  $|T| \leq 1$  implies the validity of perturbation. As far as the  $PT$ -symmetric periodic square potential in the next subsection is concerned, this statement has been checked to hold in Section II(B).

### B. $PT$ -symmetric periodic square potential

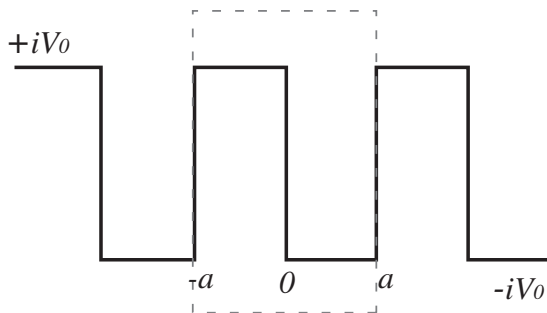


FIG. 4: A  $PT$ -symmetric periodic potential with its unit cell highlighted by the dashed line. Parameters are set at  $V_0 = 5$ ,  $a = 1$  and  $m = 1$ .

As a demonstration, we quantify our conclusions in the previous subsection for the special case of a  $PT$ -symmetric periodic square potential, as shown in Fig.4. The transmission coefficient for the unit cell can be calculated as:

$$T = \frac{t_a t_b t_c e^{i(k^+ + k^- - 2k)a}}{1 - r_a r_b e^{2ik^+ a} + r_b r_c e^{2ik^- a} - r_a r_c e^{2i(k^+ + k^-)a}} \quad (32)$$

where  $k = \sqrt{2mE}$  and  $k^\pm = \sqrt{2m(E \mp iV_0)}$  represents the momentum in the imaginary barrier/well region. The transmission and reflection amplitudes corresponding to

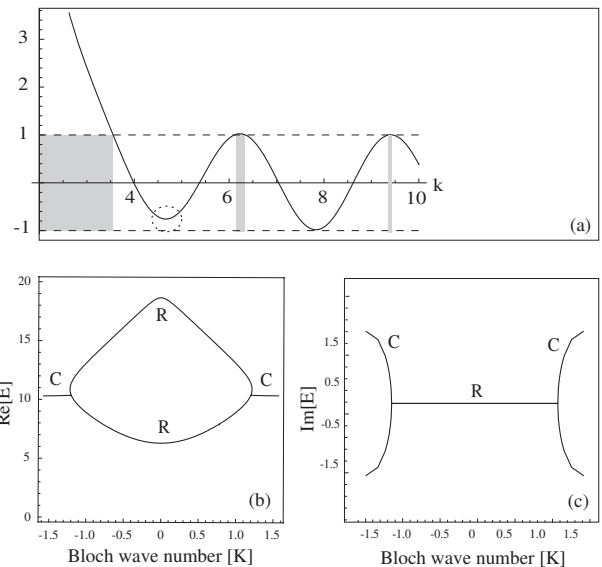


FIG. 5: (a) The RHS of Eq.(31),  $\cos(kd + \theta)/|T|$ , is shown in the solid line for the potential and parameters defined in Fig.4. There will be allowed (unshaded) and forbidden (shaded) regions of  $k$ . When  $\cos Kd$  intersects the point highlighted by the dashed circle, the corresponding  $K$  value illustrates one branch point. (b) The real part of the first dispersion band. The capital letter R/C indicates that the spectrum is real/complex in magnitude. (c) The imaginary part of the first dispersion band.

the three boundaries are denoted by  $t_a = 2k/(k + k^+)$ ,  $t_b = 2k^+/(k^+ + k^-)$ ,  $t_c = 2k^-/(k^- + k)$ ,  $r_{a,b} = 1 - t_{a,b}$  and  $r_c = t_c - 1$ .

Inserting Eq.(32) into Eq.(31) and the dispersion relation can be determined as:

$$\cos(k^+ + k^-)a - \frac{(k^+ - k^-)^2}{2k^+ k^-} \sin k^+ a \sin k^- a = \cos 2Ka. \quad (33)$$

The band structure is solved numerically and plotted in Fig.5.

The perturbation method has been demonstrated to break down for a single localized complex barrier potential in Section II(B), either with or without an accompanying well. When it is generalized to a  $PT$ -symmetric periodic potential, we are sure that the perturbation remains at fault from the analysis within one unit cell. In the meantime, Fig.5 shows that the originally real eigenenergies evolve into both complex and real spectra. So the existence of branch points and the breakdown of perturbation are tied together as proved by Ref.[10]. In the mean time, the values of  $|T|$  at these extrema also become greater than unity, as is shown in Tab.II.

In passing, we observed a special bond between the branch points and the Fano resonances discussed in Section II(B). Since the momenta  $k^+$  and  $k^-$  here happen to be complex conjugates when  $E$  is real, the reflection amplitude in Eq.(14) is rendered pure imaginary. The condition for constructive interference becomes identical

$E$	10.39	30.62	60.34	99.87
$ T $	1.36	1.02	1.00	1.00
$n + 1/2$	1.50	2.50	3.50	4.50

TABLE II: Partial list of energies and absolute magnitude of the transmission amplitude at the branch points. Their corresponding resonance numbers  $n$  from  $n + 1/2 = 2a/\lambda = a\sqrt{2mE}/\pi$  indeed are close to integers.

to Eq.(13). This is supported by the numerical results for the branch points presented in Tab.II, which indeed approach those for the resonances.

#### IV. DISCUSSIONS AND CONCLUSIONS

Since the non-Hermitian potential results from our examining an open system which is allowed to exchange particles with its environment, the conventional continuity equation is no longer obeyed[11, 13, 14, 15]. One interesting debate[16] is whether it is meaningful to mend this loss of unitarity. Several studies[16, 17, 18] have been devoted to this effort. They tried to construct a metric and corresponding transformed wave function as the general framework[19, 20, 21, 22, 23] to examine the subsystem in a quasi-Hermitian analysis. Although the

unitarity can be restored, one is constrained to discuss wavefunctions either coming simultaneously from both sides[16, 17] or exhibiting different normalization constants on either side of the potential[18]. To resolve these dilemmas, Jones[17] suggested that one simply treats the non-Hermitian scattering potential as an effective one in the standard framework of quantum mechanics. This is the view we adopt in this work at studying the localized NH potentials as a phenomenological model of a quantum sink or source in an open system.

In conclusion, although the breakdown of perturbation approach has been identified to be intimately linked to the existence of complex spectrum for a  $PT$ -symmetric periodic potential, we offer new insights into their relationship by studying the less sophisticated case of an imaginary barrier potential. Due to the simplicity of this potential form, we are able to elucidate the cause of the similar breakdown of perturbation, why the perturbation can be remedied by the superimposition of a sufficiently large real potential, and the condition for a constructive interference which differs from that for a real potential. Most importantly, we provide a more comprehensive criteria through Eq.(31) on why, when and where the bifurcation will occur.

We thank Hsiu-Hau Lin for useful comments and acknowledge the support by NSC in Taiwan under grant No. 95-2112-M007-046-MY3.

- 
- [1] C. M. Bender and S. Boettcher, Phys. Rev. Lett. **80**, 5243 (1998).  
[2] C. M. Bender, Contemp. Phys. **46**, 277 (2005).  
[3] A. Mostafazadeh, Ann. Phys. (N.Y.) **309**, 1 (2004).  
[4] C. M. Bender, Rep. Prog. Phys. **70**, 947 (2007).  
[5] C. M. Bender, D. C. Brody, H. F. Jones, and B. K. Meister, Phys. Rev. Lett. **98**, 040403 (2007).  
[6] A. Mostafazadeh, Phys. Rev. Lett. **99**, 130502 (2007).  
[7] P. Dorey, C. Dunning, and R. Tateo, J. Phys. A: Math. Gen. **34**, 5679 (2001).  
[8] Z. H. Musslimani, K. G. Makris, R. El-Ganainy, and D. N. Christodoulides, Phys. Rev. Lett. **100**, 030402 (2008).  
[9] K. G. Makris, R. El-Ganainy, and D. N. Christodoulides, and Z. H. Musslimani, Phys. Rev. Lett. **100**, 103904 (2008).  
[10] S. Klaiman, U. Günther, and N. Moiseyev, Phys. Rev. Lett. **101**, 080402 (2008).  
[11] F. Cannata, J-P. Dedonder, and A. Ventura, Ann. Phys. (N.Y.) **322**, 397 (2007).  
[12] I. Gilary, A. Fleischer, and N. Moiseyev, Phys. Rev. A. **72**, 012117 (2005).  
[13] Z. Ahmed, Phys. Lett. A. **324**, 152 (2004).  
[14] Z. Ahmed, C. M. Bender, and M. V. Berry, J. Phys. A: Math. Gen. **38**, L627 (2005).  
[15] M. Znojil, J. Phys. A: Math. Gen. **39**, 13325 (2006).  
[16] H. F. Jones, Phys. Rev. D. **76**, 125003 (2007).  
[17] H. F. Jones, Phys. Rev. D. **78**, 065032 (2008).  
[18] M. Znojil, Phys. Rev. D. **78**, 025026 (2008).  
[19] C. M. Bender, D. C. Brody, and H. F. Jones, Phys. Rev. Lett. **89**, 270401 (2002); *ibid.* **92**, 119902(E) (2004).  
[20] A. Mostafazadeh, J. Math. Phys. (N.Y.) **43**, 205 (2002).  
[21] H. F. Jones, J. Phys. A: Math. Gen. **38**, 1741 (2005).  
[22] A. Mostafazadeh, J. Phys. A: Math. Gen. **38**, 6557 (2005); *ibid.* **38**, 8185(E) (2005).  
[23] H. F. Jones and J. Mateo, Phys. Rev. D **73**, 085002 (2006).